JACS
JOURNAL OF THE AMERICAN CHEMICAL SOCIETY
Communication
pubs.acs.org/JACS

Self-Assembly of Nanometer-Sized Boroxine Cages from Diboronic Acids

Kosuke Ono,[†,§] Kohei Johmoto,[‡,§] Nobuhiro Yasuda,[∥] Hidehiro Uekusa,[‡,§] Shintaro Fujii,[†] Manabu Kiguchi,[†] and Nobuharu Iwasawa*[,†,§]

[†]Department of Chemistry, [‡]Department of Chemistry and Materials Science, Tokyo Institute of Technology and [§]JST-CREST, O-okayama, Meguro-ku, Tokyo 152-8551, Japan

[∥]Japan Synchrotron Radiation Research Institute/SPring-8, 1-1-1 Kouto, Sayo-cho, Sayo-gun, Hyogo 679-5198, Japan

Supporting Information

ABSTRACT: By use of the reversible trimerization of boronic acids, the series of boroxine cages **3-mer**, **6-mer**, and **12-mer** were constructed from rationally designed diboronic acids whose bond angles between two C−B bonds are 60°, 84°, and 117°, respectively. Boroxine cages **6-mer** and **12-mer** have 1.5 and 2.5 nm sized cavities, respectively.

Boroxines, trimeric six-membered-ring compounds $(RB-O)_3$, are formed reversibly by the dehydration of three molecules of boronic acid and show high thermal stability and Lewis acidity.[1] Utilizing this unique reversible trimerization, boroxine formation with monoboronic acids has been applied to the construction of tripodal molecular architectures such as star polymers,[2] dendrimers,[3] [4]rotaxanes,[4] octupolar molecules as potential candidates for nonlinear optical (NLO) materials,[5] etc.[6] (Scheme 1a). In addition, polymeric boroxine networks have been prepared by using di-, tri-, or tetraboronic acids to afford potential boroxine-based organic materials such as porous crystalline materials (covalent organic frameworks (COFs)),[7] flame-retardant materials,[8] anion-trapping materials in lithium ion batteries,[9] etc.[10] (Scheme 1b). On the other hand, the formation of discrete molecular architectures by means of boroxine formation, where a precise number of boroxines is involved, has rarely been developed in spite of their high possibility to realize novel boroxine-based architectures and materials.[11] We have explored the construction of cage architectures through dehydration of diboronic acids, where two phenylboronic acid moieties are appropriately positioned (Scheme 1c).[12] Herein we report the self-assembly of a series of nanometer-sized boroxine cages by simple dehydration of rationally designed diboronic acids.

Scheme 1. Boroxine-Based (a) Tripodal, (b) Network, and (c) Cage Architectures

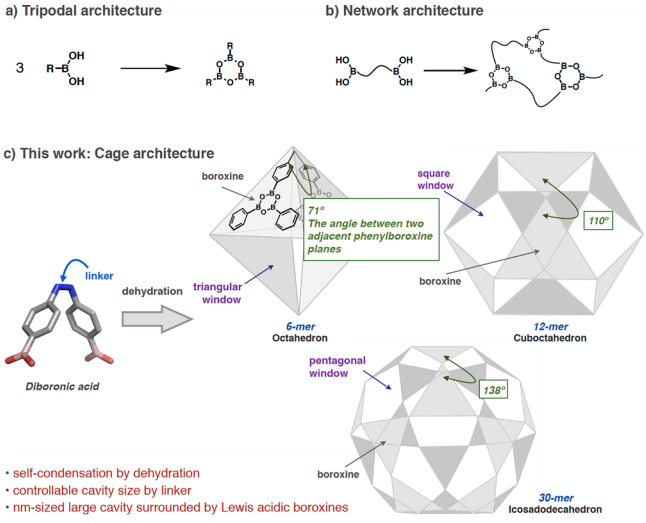

To address the anticipated challenge of controlling the degree of oligomerization, a delicate choice of the framework of the diboronic acid is required. It was expected that three cage architectures would be possible by boroxine formation from diboronic acids (Scheme 1c),[11] namely, octahedral, cuboctahedral, and icosadodecahedral cages, which correspond to **6-mer**, **12-mer**, and **30-mer** of diboronic acids. These cages are composed of triangular phenylboroxine moieties with triangular, square, or pentagonal windows, respectively. If the window extends to hexagonal, a planar network architecture known as COF-1[7a] could be constructed. To control the formation of these cage structures, the design of the diboronic acid, in particular the angle between the two adjacent phenylboroxine planes, is the most important. The ideal angles between two C−B bonds of diboronic acids for the construction of octahedral, cuboctahedral, and icosadodecahedral cages are 71°, 110°, and 138°, respectively (Scheme 1c).[13] Therefore, a 4,5-disubstituted catechol derivative, a 3,6-disubstituted carbazole derivative, a 2,4-disubstituted resorcinol derivative, and a 2,5-disubstituted thiophene derivative were selected as frameworks, and diboronic acids **1**, **2**, **3**, and **4** with estimated angles of 66°, 84°, 117°, and 148°, respectively, between the two C−B bonds (Figure 1; also see Figure S1 in the Supporting Information (SI)) were prepared for the construction of these cages.[14,15] The facile introduction of long alkyl chains to increase the solubility of the boroxine cages is possible for these frameworks.

First, boroxine formation of diboronic acid **1**, whose angle between the two C−B bonds is a little smaller than ideal angle for the octahedral cage, was examined (Figure 2a). Diboronic

Received: March 15, 2015
Published: May 18, 2015

DOI: 10.1021/jacs.5b02716
J. Am. Chem. Soc. 2015, 137, 7015−7018

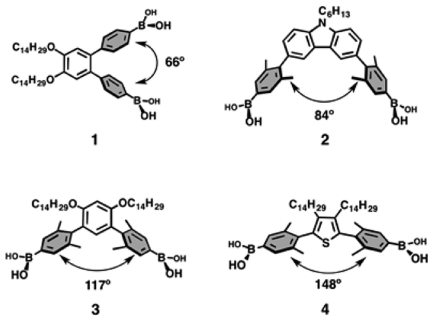

Figure 1. Estimated bond angles of diboronic acids **1**, **2**, **3**, and **4**.

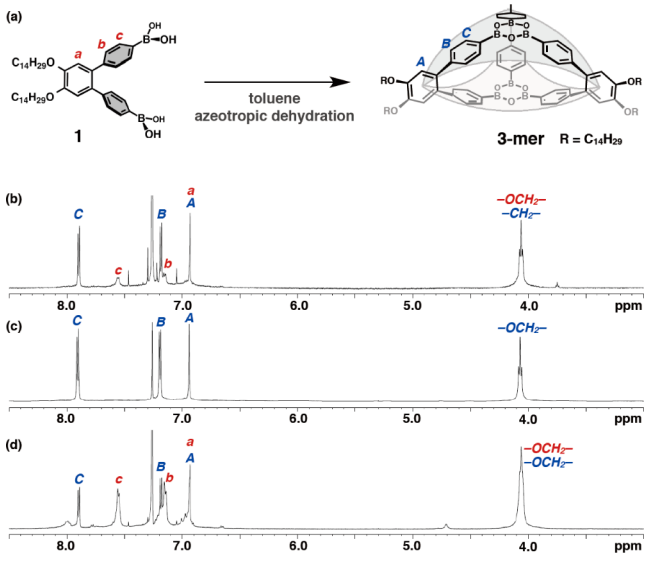

Figure 2. (a) Self-assembly of boroxine cage **3-mer**. (b–d) Partial ^{1}H NMR spectra (500 MHz, $CDCl_3$, rt) of (b) the solution right after the dissolution of diboronic acid **1**, (c) boroxine cage **3-mer** after azeotropic dehydration, and (d) the solution after the addition of D_2O.

acid **1** is soluble in $CDCl_3$, and the spectrum showed a set of sharp signals along with several broadened peaks (Figure 2b).[16] After azeotropic dehydration of a toluene solution of this mixture, the broadened peaks disappeared and only the sharp signals were observed, suggesting quantitative formation of a single highly symmetric discrete boroxine architecture (Figure 2c). Upon addition of D_2O to this chloroform solution, the boroxine broke down to the boronic acids, and a mixture similar to the initial material again appeared (Figure 2d). Thus, the reversibility of the boroxine formation was demonstrated. Formation of the single boroxine product was confirmed by the observation of a single peak in the gel-permeation chromatography (GPC) analysis. The molecular ion peak at m/z 2119, corresponding to the molecular weight of **3-mer**, was clearly observed by field-desorption time of flight (TOF) mass spectrometry (MS) analysis. Together with the data that will be discussed later, the boroxine formed from diboronic acid **1** is thought to be **3-mer** instead of the expected **6-mer**. From the molecular modeling study, **3-mer** should contain distorted phenylboroxine moieties (see Figure S3), and the ^{11}B NMR signal of **3-mer** was shifted upfield by 10 ppm relative to that of tolylboroxine, whose boron center is trigonal-planar.[17]

Next, boroxine formation from diboronic acid **2**, which has an angle of 84° between the two C–B bonds, was examined. Diboronic acid **2** is not soluble in toluene but dissolves in chloroform, and quantitative boroxine formation was confirmed by ^{1}H NMR spectroscopy upon heating at 60 °C in the presence of 4 Å molecular sieves (Figure 3c). High-resolution

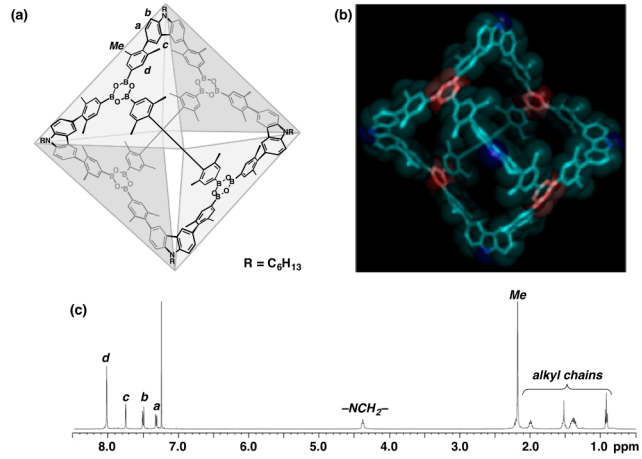

Figure 3. (a) Chemical structure, (b) single-crystal structure, and (c) ^{1}H NMR spectrum (500 MHz, $CDCl_3$, rt) of boroxine cage **6-mer**.

MALDI-Spiral TOF MS analysis of the boroxine clearly showed the formation of the boroxine cage **6-mer** (see the SI). Single crystals of **6-mer** were successfully prepared from slow vapor diffusion of *n*-hexane into a 4-bromoanisole solution, and the crystal structure (determined with synchrotron X-ray sources at SPring-8) was found to have the expected octahedral structure. The hexyl groups and solvent molecules could not be assigned because of the severe disorder, and the SQUEEZE procedure was performed in the analysis (Figure 3b). The distance between diagonal nitrogens is 2.8 nm, and the size of cavity surrounded by four boroxines extends to 1.5 nm (1900 Å^3).[18]

The cuboctahedral boroxine cage **12-mer** was also successfully self-assembled from diboronic acid **3**, whose angle extends to 117°. After trials with substrates **S1** and **S2**,[19] it was found that the dihedral angle between the boronic acid-bound phenyl ring and the central benzene ring is important for the construction of discrete boroxines (see the SI), and diboronic acid **3**, in which the two phenylboronic acids are nearly perpendicular to the resorcinol unit because of the presence of the two *o*-methyl substituents, was found to give a good result. Diboronic acid **3** was not soluble in chloroform at first, but after heating for 1 day a clear solution was obtained. ^{1}H NMR and GPC analyses suggested the formation of a single discrete boroxine (Figures 4b and 5), and ^{1}H diffusion-ordered NMR spectroscopy (DOSY) analysis indicated the formation of a large boroxine cage (diffusion coefficient (D) = 0.18 m^2/Gs). The high-resolution MALDI-Spiral TOF MS analysis obviously confirmed the formation of **12-mer**. The molecular ion peak at m/z 9261.05966, corresponding to [**12-mer** + Ag]$^+$, was clearly observed, and the isotopic pattern showed good agreement with the theoretical pattern (Figure 4c). The molecular ion peak at m/z 6972, corresponding to [**9-mer** + Ag]$^+$, which is a low-symmetry cage (Figure S7), was also observed. Because of the highly symmetric ^{1}H NMR spectrum and GPC trace, this **9-mer** was thought to be generated during MS measurement. From the molecular modeling study, **12-mer** has large (2.5 nm) cavity surrounded by eight boroxines (see the SI). This cavity size is the largest class of covalent organic cages (4400 Å^3).[18,20]

Numerous attempts to obtain single crystals of **3-mer** and **12-mer** were unsuccessful. However, the relative sizes of these

DOI: 10.1021/jacs.5b02716
J. Am. Chem. Soc. 2015, 137, 7015–7018

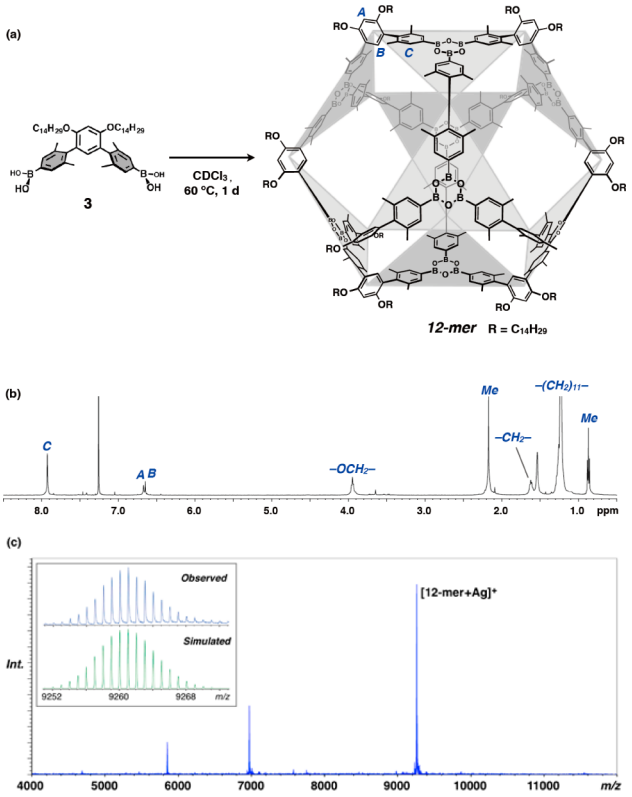

Figure 4. (a) Self-assembly of boroxine cage **12-mer** from diboronic acid **3**. (b) ^{1}H NMR spectrum (500 MHz, $CDCl_3$, rt) of boroxine cage **12-mer**. (c) MALDI-Spiral TOF MS spectrum of **12-mer** + Ag^+ (DCTB matrix; AgTFA additive). The inset shows the observed and simulated isotopic patterns of the [**12-mer** + Ag]$^+$ peak.

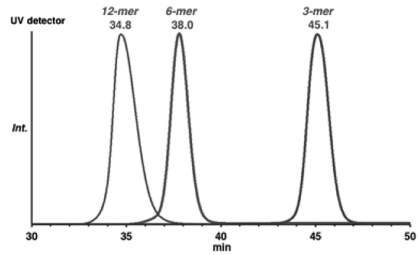

Figure 5. GPC traces of boroxine cages **3-mer**, **6-mer**, and **12-mer** by UV detector.

boroxine cages were successfully compared by several other methods.[21] First, the GPC retention times decreased in the order **3-mer** > **6-mer** > **12-mer** (Figure 5), and this tendency is consistent with the ^{1}H DOSY study, where the diffusion constants of **3-mer**, **6-mer**, and **12-mer** were found to be 0.28, 0.26, and 0.18 m^2/Gs, respectively. These results indicated that the relative sizes of the nanometer-sized boroxine cages were in agreement with modeling study. Direct observation of the boroxine cages was also performed by scanning tunneling microscopy (STM). The samples for STM measurements were prepared by placing 10 pL of molecular solution (1 mg in 1 mL of chloroform) on a Au(111) substrate. In STM images, nanometer-sized protrusions, which are thought to correspond to boroxine cages, were observed under ambient conditions at room temperature (rt).[22] The height profiles (~0.3 nm for **3-mer**, ~0.50 nm for **6-mer**, and ~0.85 nm for **12-mer**) clearly show the relative height difference among the three boroxine cages (Figure 6).[23] Thermal stability up to 300 °C for all of the

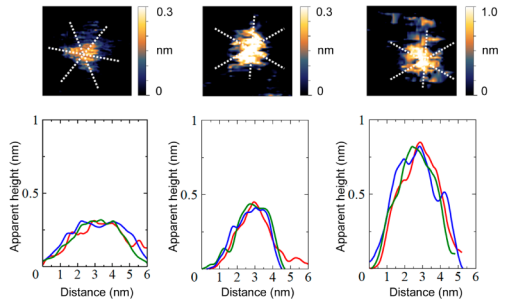

Figure 6. STM images and height profiles from three directions for boroxine cages **3-mer** (left), **6-mer** (middle), and **12-mer** (right).

boroxine cages was observed by thermogravimetric analysis and differential scanning calorimetry, in which prominent weight loss or decomposition below 300 °C was not observed.

Lastly, the formation of the icosadodecahedral boroxine cage from diboronic acid **4** was examined. Boroxine formation was tested in various solvents such as chloroform, toluene, 1,4-dioxane, THF, pyridine, or mixed solvent systems, but no evidence for the formation of boroxine cage **30-mer** was obtained by NMR, GPC, or MS analysis (Table S1 in the SI).

In conclusion, we have successfully demonstrated the self-assembly of a series of nanometer-sized boroxine cages by the facile self-condensation of appropriately designed diboronic acids. This is the first example of the self-assembly of a series of polyhedral covalent organic cages from single components.[20] It is noteworthy that the size of the cage was precisely controlled by tuning the angle between the two C–B bonds in the diboronic acid,[13,24] and the largest class of covalent organic cage, **12-mer**, was obtained from diboronic acid **3**.[18,20] It should also be emphasized that the boroxine cages **3-mer**, **6-mer**, and **12-mer** have unique cavities surrounded by two, four, and eight Lewis acidic boroxines, respectively. The results obtained here show the possibility of boroxine formation for the construction of novel cage architectures in addition to tripodal and network architectures. Further studies of the construction of the remaining boroxine cage **30-mer** and application of the boroxine cages are now in progress in our group.

■ ASSOCIATED CONTENT

Ⓢ Supporting Information

Additional experimental details, characterization data for new compounds, and crystallographic data (CIF). The Supporting Information is available free of charge on the ACS Publications website at DOI: 10.1021/jacs.5b02716.

■ AUTHOR INFORMATION

Corresponding Author

*niwasawa@chem.titech.ac.jp

Notes

The authors declare no competing financial interest.

■ ACKNOWLEDGMENTS

We thank Ms. N. Watanabe for performing MALDI-TOF MS analysis. This work was supported by a Core Research for Evolutional Science and Technology (CREST) project from the Japan Science and Technology Agency (JST). The synchrotron radiation experiments were performed on BL40XU and BL02B1 at SPring-8 with the approval of the Japan Synchrotron Radiation Research Institute (JASRI) (Proposals 2013A1052, 2014A1016, and 2014B1004).

DOI: 10.1021/jacs.5b02716
J. Am. Chem. Soc. 2015, 137, 7015–7018

REFERENCES

(1) For reviews of boroxine chemistry, see: (a) Korich, A. L.; Iovine, P. M. *Dalton Trans.* **2010**, *39*, 1423−1431. (b) Cheng, F.; Jäkle, F. *Polym. Chem.* **2011**, *2*, 2122−2132. (c) *Boronic Acids: Preparation and Applications in Organic Synthesis, Medicine and Materials*, 2nd ed.; Hall, D. G., Ed.; Wiley-VCH: Weinheim, Germany, 2011. (d) Tokunaga, Y. *Heterocycles* **2013**, *87*, 991−1021. (e) Saha, M. L.; De, S.; Pramanik, S.; Schmittel, M. *Chem. Soc. Rev.* **2013**, *42*, 6860−6909.

(2) (a) Qin, Y.; Cui, C.; Jäkle, F. *Macromolecules* **2007**, *40*, 1413−1420. (b) De, P.; Gondi, S. R.; Roy, D.; Sumerlin, B. S. *Macromolecules* **2009**, *42*, 5614−5621. (c) Korich, A. L.; Walker, A. R.; Hincke, C.; Stevens, C.; Iovine, P. M. *J. Polym. Sci. A, Part A: Polym. Chem.* **2010**, *48*, 5767−5774.

(3) Perttu, E. K.; Arnold, M.; Iovine, P. M. *Tetrahedron Lett.* **2005**, *46*, 8753−8756.

(4) Tokunaga, Y.; Ito, T.; Sugawara, H.; Nakata, R. *Tetrahedron Lett.* **2008**, *49*, 3449−3452.

(5) Alcaraz, G.; Euzenat, L.; Mongin, O.; Katan, C.; Ledoux, I.; Zyss, J.; Blanchard-Desce, M.; Vaultier, M. *Chem. Commun.* **2003**, 2766−2767.

(6) (a) Post, E. W.; Cooks, R. G.; Kotz, J. C. *Inorg. Chem.* **1970**, *9*, 1670−1677. (b) Elschenbroich, C.; Wolf, M.; Pebler, J.; Harms, K. *Organometallics* **2004**, *23*, 454−459. (c) Thilagar, P.; Chen, J.; Lalancette, R. A.; Jäkle, F. *Organometallics* **2011**, *30*, 6734−6741. (d) Ishikawa, K.; Kameta, N.; Masuda, M.; Asakawa, M.; Shimizu, T. *Adv. Funct. Mater.* **2014**, *24*, 603−609.

(7) (a) Côté, A. P.; Benin, A. I.; Ockwig, N. W.; O'Keeffe, M.; Matzger, A. J. *Science* **2005**, *310*, 1166−1170. (b) El-Kaderi, H. M.; Hunt, J. R.; Mendoza-Cortés, J. L.; Côté, A. P.; Taylor, R. E.; O'Keeffe, M.; Yaghi, O. M. *Science* **2007**, *316*, 268−272. (c) Wan, S.; Guo, J.; Kim, J.; Ihee, H.; Jiang, D. *Angew. Chem., Int. Ed.* **2009**, *48*, 5439−5442. For recent reviews of COFs, see: (d) Feng, X.; Ding, X.; Jiang, D. *Chem. Soc. Rev.* **2012**, *41*, 6010−6022. (e) Ding, S.-Y.; Wang, W. *Chem. Soc. Rev.* **2013**, *42*, 548−568.

(8) Morgan, A. B.; Jurs, J. L.; Tour, J. M. *J. Appl. Polym. Sci.* **2000**, *76*, 1257−1268.

(9) (a) Mehta, M. A.; Fujinami, T. *Chem. Lett.* **1997**, *26*, 915−916. (b) Yang, Y.; Inoue, T.; Fujinami, T.; Mehta, M. A. *Solid State Ionics* **2001**, *140*, 353−359. (c) Forsyth, M.; Sun, J.; Zhou, F.; MacFarlane, D. R. *Electrochim. Acta* **2003**, *48*, 2129−2136.

(10) (a) Li, Y.; Ding, J.; Day, M.; Tao, Y.; Lu, J.; D'iorio, M. *Chem. Mater.* **2003**, *15*, 4936−4943. (b) Bunck, D. N.; Dichtel, W. R. *Angew. Chem., Int. Ed.* **2012**, *51*, 1885−1889. (c) Kalidindi, S. B.; Oh, H.; Hirscher, M.; Esken, D.; Wiktor, C.; Turner, S.; Tendeloo, G. V.; Fischer, R. A. *Chem.—Eur. J.* **2012**, *18*, 10848−10856. For a review of 2D boroxine networks on metal surfaces, see: (d) Clair, S.; Abel, M.; Porte, L. *Chem. Commun.* **2014**, *50*, 9627−9635.

(11) To the best of our knowledge, there has been only one report that utilized oligomeric boroxine formation for the construction of molecular architecture. In that report, ferrocene−boroxine cyclophane was prepared from 1,1′-ferrocenediboronic acid, and the possibility of boroxine-based polyhedra was also discussed. See: Chen, T.-H.; Kaveevivitchai, W.; Bui, N.; Miljanić, O. Š. *Chem. Commun.* **2012**, *48*, 2855−2857.

(12) There has been one report on the synthesis of a cage structure by the combination of boroxine formation and dative B−N interaction from 3-pyridylboronic acid. However, the cage did not seem to have enough room to include guest molecules. See: Salazar-Mendoza, D.; Guerrero-Alvarez, J.; Höpfl, H. *Chem. Commun.* **2008**, 6543−6545.

(13) In the synthesis of spherical complexes by coordination bonding, the ligand bend angle determines the final product. See: Harris, K.; Fujita, D.; Fujita, M. *Chem. Commun.* **2013**, *49*, 6703−6712.

(14) These angles were calculated from the optimized structure by molecular mechanics calculations (MMFF) using Spartan. In the calculations, long alkyl chains were replaced by methyl groups.

(15) Diboronic acids are known to exist as mixtures of acid and anhydride forms in the solid state. Also see ref 1c.

(16) In solution, an equilibrium mixture of boronic acid and boroxine was observed. See: Tokunaga, Y.; Ueno, H.; Shimomura, Y.; Seo, T. *Heterocycles* **2002**, *57*, 787−790.

(17) Similar upfield shifts of the ^{11}B NMR signals were observed for **6-mer** and **12-mer**, where the phenylboroxine moieties are not planar in the modeling study. Ligation to boron by a base such as water was not clearly observed in the NMR spectrum.

(18) The volumes of **6-mer** and **12-mer** were estimated from the inside octahedron with an edge length of 16.0 Å or cuboctahedron with an edge length of 12.3 Å, respectively. For a size comparison of the largest class of covalent organic cages, see the Supporting Information.

(19) Diboronic acids **S1** and **S2** have a bond angle of ca. 120° between the two C−B bonds but different dihedral angles between the boronic acid-bound phenyl ring and the central benzene ring. While **S1** did not give any discrete boroxine, **S2**, which has a larger dihedral angle, gave a discrete boroxine partially. See the Supporting Information for details.

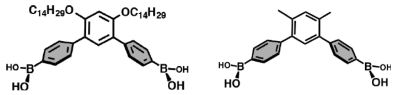

S1 S2

(20) For examples of the largest class of covalent organic cages, see: (a) Liu, Y.; Liu, X.; Warmuth, R. *Chem.—Eur. J.* **2007**, *13*, 8953−8959. (b) Jelfs, K. E.; Wu, X.; Schmidtmann, M.; Jones, J. T. A.; Warren, J. E.; Adams, D. J.; Cooper, A. I. *Angew. Chem., Int. Ed.* **2011**, *50*, 10653−10656. (c) Skowronek, P.; Warżajtis, B.; Rychlewska, U.; Gawroński, J. *Chem. Commum.* **2013**, *49*, 2524−2526. (d) Zhang, G.; Presly, O.; White, F.; Oppel, I. M.; Mastalerz, M. *Angew. Chem., Int. Ed.* **2014**, *53*, 1516−1520. For reviews of covalent organic cages in which most of the polyhedral cages were constructed by imine or boronic ester formation using two components, see: (e) Cooper, A. I. *Angew. Chem., Int. Ed.* **2012**, *51*, 7892−7894. (f) Mastalerz, M. *Chem.—Eur. J.* **2012**, *18*, 10082−10091. (g) Jin, Y.; Zhu, Y.; Zhang, W. *CrystEngComm* **2013**, *15*, 1484−1499. (h) Zhang, G.; Mastalerz, M. *Chem. Soc. Rev.* **2014**, *43*, 1934−1947. (i) Jin, Y.; Wang, Q.; Taynton, P.; Zhang, W. *Acc. Chem. Res.* **2014**, *47*, 1575−1586.

(21) **3-mer**, **6-mer**, and **12-mer**, which have the same alkyl chains (R = $C_{14}H_{29}$), were used for the comparison of the relative sizes. **6-mer** (R = $C_{14}H_{29}$) was prepared in the same manner as **6-mer** (R = C_6H_{13}), whose structure was determined by single-crystal X-ray diffraction. See the Supporting Information for details.

(22) It is not clear whether a boroxine or a window faces the Au surface. However, because of the high symmetry of the boroxine cages, the height profiles among boroxine cages could be compared.

(23) The apparent lateral sizes extracted from the STM images are overestimated because of the tip convolution effect, in which the tip shape is convoluted into the STM images.[25] On the other hand, the reduced apparent height of the boroxine cages with respect to the physical height can be ascribed to tip-induced deformation for the series of boroxine-based architectures during STM imaging. For further details, see the Supporting Information.

(24) In the synthesis of imine cages with aliphatic linkers, the cage size was controlled by the function of linker length. See: Jelfs, K. E.; Eden, E. G. B.; Culshaw, J. L.; Shakespeare, S.; Pyzer-Knapp, E. O.; Thompson, H. P. G.; Bacsa, J.; Day, G. M.; Adams, D. J.; Cooper, A. I. *J. Am. Chem. Soc.* **2013**, *135*, 9307−9310.

(25) Wiesendanger, R. *Scanning Probe Microscopy and Spectroscopy*; Cambridge University Press: New York, 1994.

DOI: 10.1021/jacs.5b02716
J. Am. Chem. Soc. 2015, 137, 7015−7018